JOURNAL OF APPLIED ELECTROCHEMISTRY 13 (1983) 235–243

The electrochemical study of a chromium plating bath. I. Reactions leading to solution-free species

JIANG LIN-CAI* and D. PLETCHER

Department of Chemistry, The University, Southamptom SO9 5NH, UK

Received 18 March 1982

The electrode reactions occurring at C, Cr, Cu and Ni cathodes in the standard electroplating solution for chromium, 200 g dm^{-3} CrO_3 and 2 g dm^{-3} H_2SO_4, have been reinvestigated. This paper emphasises the study of those reactions which lead to solution-free products; these occur at potentials positive to that necessary for film or metal deposition. For each cathode, the *I–E* curve shows a wave or peak for the reduction of chromium (VI) to chromium(III) and it is demonstrated that this process is mass transport controlled, apparently by the transport of sulphate ions to the electrode surface. At Cr, Ni and Cu, the potential of the chromium(VI)/chromium(III) couple is determined by the removal of an insulating oxide film which forms spontaneously when the metal is immersed in the bath. In certain conditions it is also possible to define a well formed wave for proton reduction.

1. Introduction

Many metal objects, e.g. engineering and car components, household goods and kitchen utensils, are finished by the electrodeposition of chromium on to an underlayer of nickel and/or copper. The chromium deposition is commonly carried out in a plating bath containing a high concentration of chromium trioxide (200 g dm^{-3}) and a low concentration of sulphuric acid (2 g dm^{-3}) and using a high current density (200 mA cm^{-2}) [1–4]. In these conditions the current efficiency is, however, low (8–15%) because of concurrent hydrogen evolution. Moreover the mechanism of the chromium electroplating process remains unclear. Several groups have indicated the importance of a film on the electrode surface prior to the deposition of metallic chromium [5–18] while others have invoked the participation of atomic hydrogen [19]. It has also been noted that chromium metal cannot be deposited from aqueous solutions of chromic salts and that chromium(III) species are byproducts from the reduction of chromium(VI) to the metal. This has led to the proposal that chromium metal results from the reduction of chromium(VI) without intermediate oxidation states [1–4, 20].

Hence this and the following paper report further studies of some aspects of the electrochemistry of the chromium electroplating solution, chromium trioxide (200 g dm^{-3}) and dilute sulphuric acid. This paper will consider the processes which lead to solution-free intermediates while the following one will consider the evidence for a surface film and the formation of metallic chromium.

2. Experimental procedure

Three compartment cells were used throughout this work. For most experiments, a glass H-cell was used. The working electrodes were discs, area approximately 0.2 cm^2, mounted in PTFE or in the case of vitreous carbon, epoxy resin, the counter electrode was a platinum wire in a compartment separated from the working electrode by a glass sinter and the reference electrode was a saturated potassium sulphate, mercury/mercurous sulphate electrode (Radiometer type K601) mounted in a Luggin probe (all potentials in this paper are quoted versus this electrode). The Cu and Ni disc electrodes were prepared from Specpure rods (Johnson Matthey Ltd) and the C discs from vitreous carbon GC30 grade (Tokai, Japan). Before each experiment these electrodes (except

---

* On leave from the South China Teacher's University, Guangzhou, China.

0021–891X/83/020235–09$03.58/0

Cr) were polished with 1μ, then 0.5μ, alumina powder (Banner Scientific Ltd) on a damp polishing cloth and washed thoroughly with distilled water. The Cr discs were prepared by electrodeposition on to a Cu disc by applying a potential of -1.7 V for 10 s in situ in the CrO_3 solution (200 g dm^{-3}) and H_2SO_4 (2 g dm^{-3}) and used directly. For the coulometric experiments, a glass pipe cell was used. The working electrode, a vertical 2 cm^2 disc mounted in PTFE or a 2 cm^2 gauze, and the Pt gauze counter electrode entered the cell through ground glass joints at opposite ends of a glass tube with a parallel glass sinter between them; the reference electrode was again mounted in a Luggin capillary. The catholyte volume in both cells was about 20 cm^3.

The experiments used a Hi-tek Instruments potentiostat, model DT 2101, and function generator, model PPR1, and a Hewlett Packard *x–y* recorder, type 7015B. Where necessary a Gould digital storage oscilloscope, model OS 4100 was used to store transient data before transfer to the *x–y* recorder. The rotating disc experiments were carried out with an Oxford Electrodes motor and control unit.

All chemicals were Analar grade (BDH Ltd) and solutions were prepared with triply distilled water and deoxygenated in the cell with oxygen-free nitrogen (BOC Ltd). Measurements were made at room temperature, 17 ± 2° C.

3. Results and discussion

The *I–E* curve resulting from cyclic voltammetry of solutions of CrO_3 (200 g dm^{-3}) and H_2SO_4 (0.5–10 g dm^{-3}) is critically dependent on the electrode material, concentration of H_2SO_4 and the negative potential limit but it also varies with the rotation rate of the disc electrode and the potential scan rate. The subject of this paper is, however, well defined by the curve in Fig. 1 for a linear potential scan at a stationary nickel electrode. Three distinct electrode reactions, labelled A, B and C are clearly observed and a strong indication of the nature of these processes may be obtained by visual observation of the cell when the potential is held at appropriate values. At -1.0 V, the catholyte close to the nickel surface changes from dark organge to blue green, at -1.3 V vigorous gas evolution can be seen while at -1.7 V a chromium metal deposit is formed on the cathode surface. Hence it is probable that the three reactions are [7, 13]

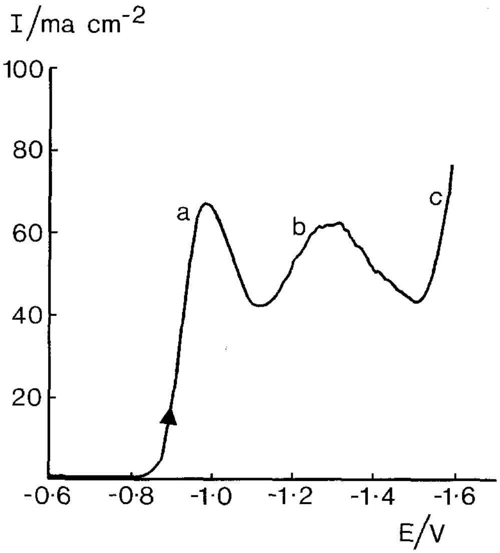

Fig. 1. *I–E* curve resulting from a linear potential sweep experiment for a Ni electrode in a solution of 200 g dm^{-3} CrO_3 + 2 g dm^{-3} H_2SO_4. Potential scan rate 0.02 V s^{-1}.

Process A $Cr(VI) + 3e \rightarrow Cr(III)$
Process B $2H^+ + 2e \rightarrow H_2$
Process C $Cr(III) + 3e \rightarrow Cr$.

Most of this paper concerns the study of peak A. The high current densities in Fig. 1 and, indeed, all the experiments in this study should be noted but are an inevitable consequence of using a practical chromium plating solution. They may, however, lead to some inaccuracy in the control of the potential due to an uncompensated IR drop.

Figure 2 shows cyclic voltammograms for each of the four electrodes studied; in each case the direction of the scan is reversed at a potential slightly negative to peak A and the electrodes are stationary. Firstly it should be noted that the potential of the first reduction process is different at the four cathodes and in particular the reduction occurs more readily by about 1 V at vitreous carbon. Secondly, the curves at the three metals show 'nucleation loops' i.e. there is a potential range where the reduction current is higher on the reverse scan than on the sweep towards negative potentials. This latter behaviour may be confirmed by potential step experiments. When the potential of the metal cathodes is pulsed from -0.6 V to

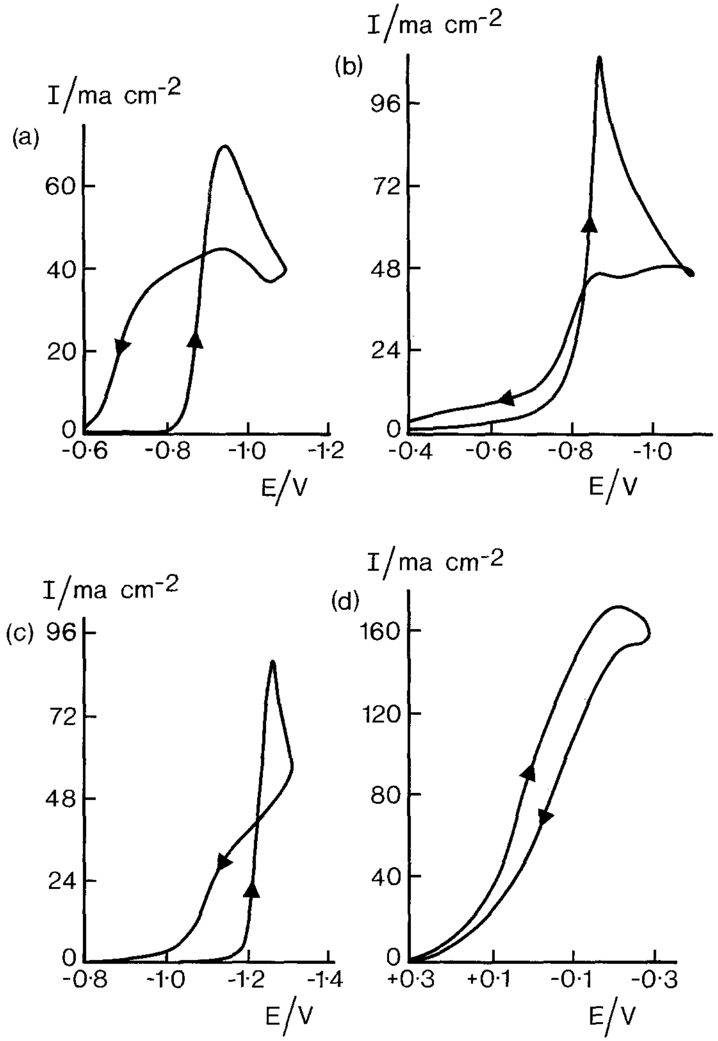

Fig. 2. Cyclic voltammograms for the solution, 200 g dm^{-3} CrO_3 + 2 g dm^{-3} H_2SO_4 at; (a), Ni; (b), Cu; (c), Cr; (d), vitreous C. In each case the direction of potential scan is reversed just beyond the first peak. At Ni, the potential scan rate is 0.02 V s^{-1}, at the other electrodes 0.03 V s^{-1}.

potentials in the foot of peak A, rising I–t transients are observed. Figure 3 shows such transients for the nickel electrode while Fig. 4 demonstrates that when this data is replotted as $I^{1/2}$ versus t, straight lines are obtained and the slopes increase as the potential is made more negative. In contrast similar experiments with a vitreous carbon electrode led to falling transients. Results such as those obtained from the cyclic voltammetric and potential step experiments with the Ni, Cu and Cr electrodes are commonly indicative of the nucleation and growth of a new conducting phase on the electrode surface. This is unlikely here if, as is confirmed below, peak A is for the reduction of Cr(VI) to Cr(III). On the other hand, when the metals are immersed in the strongly oxidising plating bath, oxidation of the metal surfaces to give a film (which inhibits the reduction of Cr(VI) to Cr(III)) is likely to occur spontaneously and rapidly. The 'nucleation loops' and rising transients would then arise by the nucleation and expansion of holes in the oxidation film during its reduction back to a clean metal surface. The reduction of Cr(VI) to Cr(III) commences as film free surface becomes available and such active areas will increase with time as the oxidation film

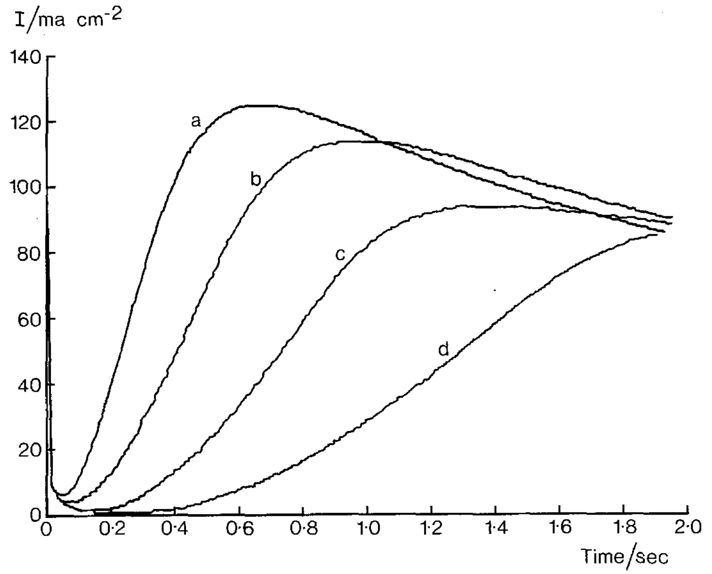

Fig. 3. *I–t* transients in response to potential steps from − 0.6 V to (a) − 0.94 V, (b) − 0.92 V, (c) − 0.90 V, (d) − 0.88 V, Ni electrodes. Solution as Figs. 1 and 2.

is removed. Certainly the shapes of the *I–t* transients are consistent with the continuous nucleation of holes in the passive film and two dimensional growth of reduced surface; the reduction of Cr(VI) to Cr(III) at the reduced surface will only serve to amplify the current at all times. In such a situation, the hysterisis in the cyclic voltammetry would be due to irreversibility in the formation and reduction of the surface film and the potentials of peak A on the cyclic voltammograms is determined by the potential for the reduction of the passivating film on each of the metals. The contrasting behaviour of vitreous carbon suggests that it does not spontaneously form an oxide film in the CrO_3 solution and certainly the potential of peak A is, at this electrode, closer to that expected for a Cr(VI)/Cr(III) couple.

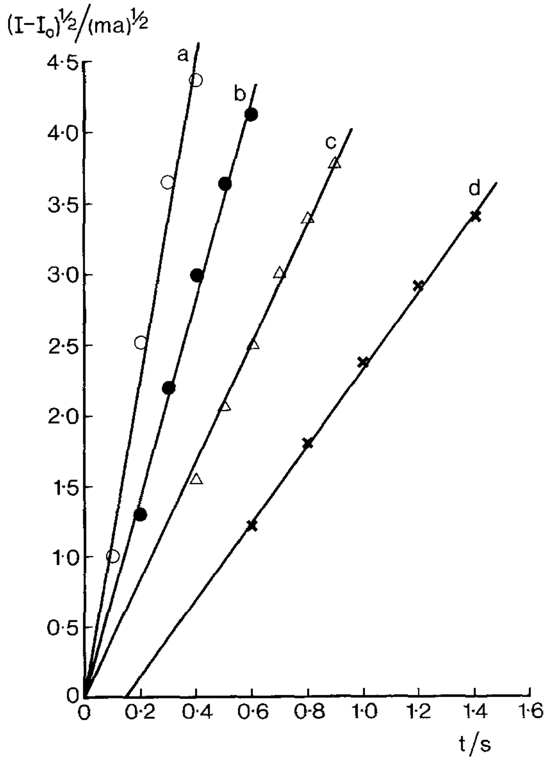

Fig. 4. *I–t* response of Fig. 3 replotted as $(I - I_0)^{1/2}$ versus t plots. I_0 is the current just before the I increases with t. (a) − 0.94 V, (b) − 0.92 V, (c) − 0.90 V, (d) − 0.88 V.

In order to confirm the electrode reaction giving rise to peak A on the cyclic voltammograms, a series of controlled potential electrolyses with large cathodes were carried out. The electrolyses were terminated after the passage of a low charge so that the Cr(VI) concentration in the electrolyte did not undergo a substantial change and the chromium(III) formed and present in solution was estimated gravimetrically [1]. The results are reported in Table 1 and it can be seen that the Cr(III) found is close to that expected on the basis of Faraday's law confirming that the electrode reaction is the simple reduction of Cr(VI) to Cr(III) as a solution free species.

Figure 5 illustrates the effect of potential scan rate and sulphate ion concentration on peak A. The cyclic voltammograms are for a copper electrode

Table 1. Comparison of the weight of chromium(III) formed in solution during controlled potential electrolysis and estimated gravimetrically with that expected on the basis of Faraday's law.

Cathode	*E* (V)	*Charge passed* (C)	*Cr(III) formed* (g)	
			Experimental	*Theoretically*
Cu	-0.9	447	0.081	0.080
Cu	-1.0	716	0.125	0.129
Ni	-1.0	592	0.094	0.106
C	-1.0	181	0.033	0.032

with various H_2SO_4 concentrations but similar results could be obtained for C, Ni and Cr electrodes and for solutions prepared with 1 g dm^{-3} H_2SO_4 and variable Na_2SO_4 concentrations.

Although the reverse scans are not shown in the figure, all except those at C show nucleation loops and there is never an anodic peak for the reoxidation of Cr(III) to Cr(VI). The Cr(VI)/Cr(III) couple is very irreversible. It can be seen from the figure that the currents in peak A depend strongly on both potential scan rate and sulphate concentration and although neither $I_p/v^{1/2}$ or $I_p/C_{SO_4^{2-}}$ are quite constant the data suggests that the peak current for the Cr(VI)/Cr(III) process is largely mass transport controlled and that the concentration of sulphate influences the flux of electroactive species. This conclusion can be confirmed using either potential step or rotating disc techniques provided the potentials are selected carefully for each electrode material (see later). It is also in accord with an earlier observation that the

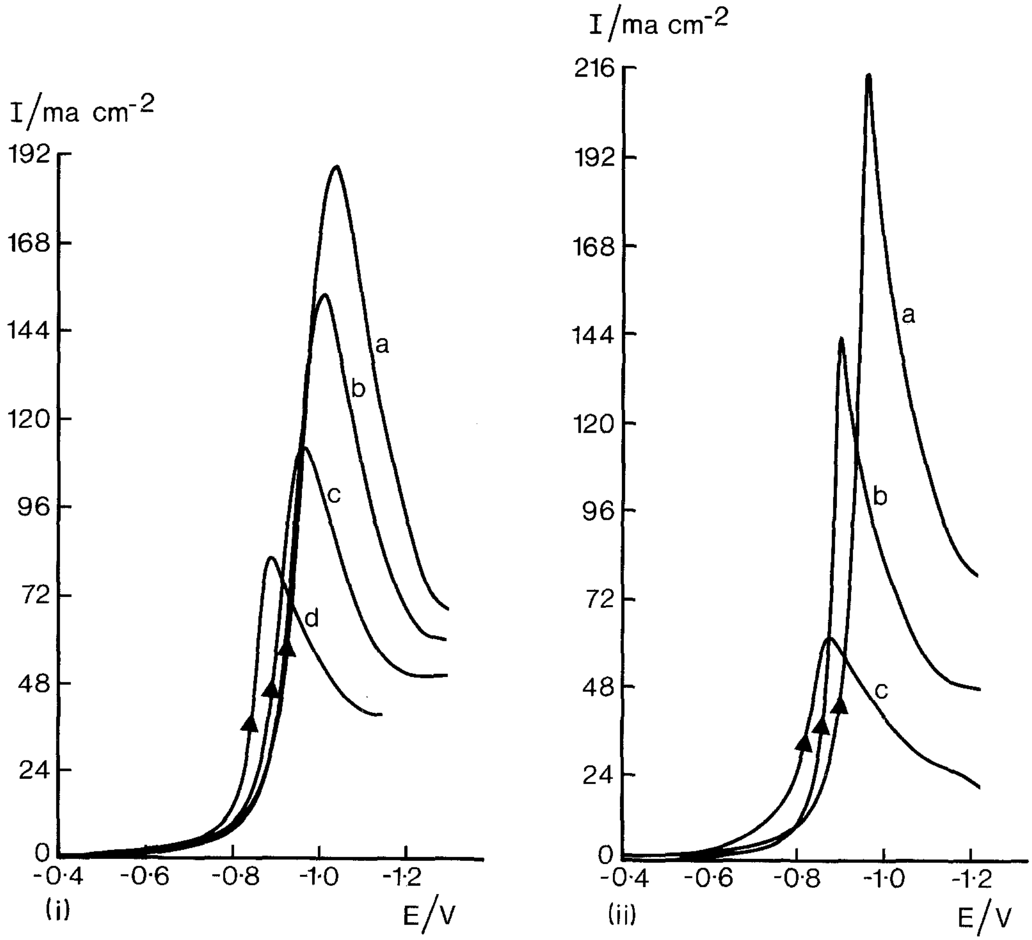

Fig. 5. *I–E* curves from linear potential sweep experiments. Cu electrode. i, effect of potential scan rate (a) 0.2 V s^{-1}, (b) 0.1 V s^{-1}, (c) 0.05 V s^{-1}, (d) 0.02 V s^{-1}. Solution; 200 g dm^{-3} CrO_3 + 2 g dm^{-3} H_2SO_4. ii, effect of sulphate concentration; potential scan rate 0.05 V s^{-1}. (a) 4 g dm^{-3}, (b) 2 g dm^{-3}, (c) 1 g dm^{-3} H_2SO_4. Solution also contains 200 g dm^{-3} CrO_3.

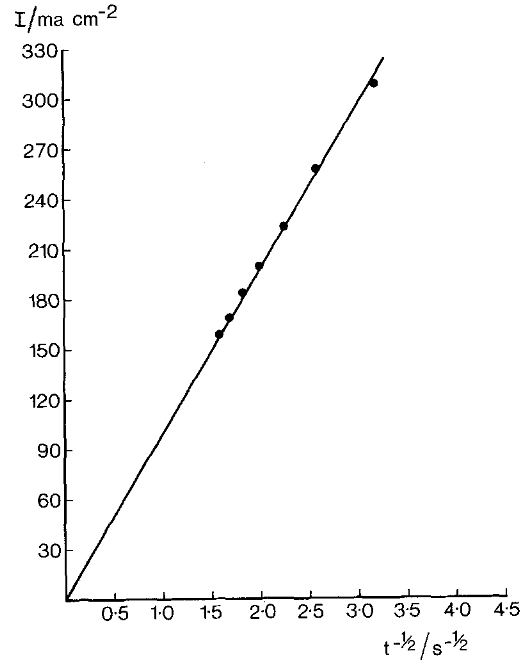

Fig. 6. I versus $t^{-1/2}$ plot for I–t response to a potential step from – 0.4 V to – 1.2 V. Cu electrode. Solution as Fig. 1.

first stage of a galvanostatic reduction is diffusion controlled [23]. For example, Fig. 6 shows the linear I–$t^{-1/2}$ plot replotted from the falling part at times beyond the peak of an I–t transient recorded in response to a potential step from – 0.4 V to – 1.2 V at a Cu electrode. Figure 7 shows I–$\omega^{1/2}$ plots for a rotating chromium electrode in solutions of CrO_3 (200 g dm^{-3}) and three different sulphate concentrations. Moreover assuming that it is the transport of sulphate to the electrode which determines the current, the values of diffusion coefficient calculated from the slopes of Figs. 6 and 7 are close to the expected value (from the potential step experiment $D_{SO_4^{2-}} = 0.93 \times 10^{-5}$ cm^2 s^{-1} and from the rotating disc experiment the values of $D_{SO_4^{2-}}$ found were 1.3×10^{-5}, 1.6×10^{-5} and 1.1×10^{-5} cm^2 s^{-1}). Of course, any calculation assuming that transport of the total Cr(VI) species to the electrode is the rate determining step would lead to an unreasonably low value for the diffusion coefficient. All this data is consistent with a model where the current for Cr(VI) to Cr(III) is determined by the transport of SO_4^{2-} simply because of the need to maintain charge balance at the cathode surface as Cr^{3+} is formed; the chromium containing anions cannot perform this function, at least

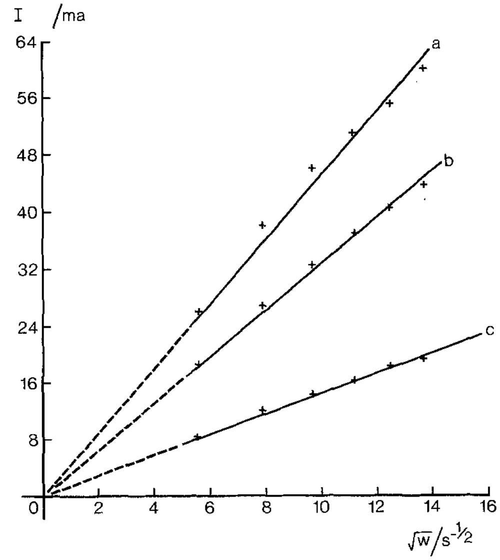

Fig. 7. I versus $\omega^{1/2}$ plots for a rotating Cr electrode in solutions of 200 g dm^{-3} CrO_3 containing (a) 6 g dm^{-3} H_2SO_4, (b) 4 g dm^{-3} H_2SO_4, (c) 2 g dm^{-3} H_2SO_4.

at these potentials, because the species formed are not soluble. It cannot be ruled out, however, that it is the transport of a minor Cr(VI) species which controls the current, but other Cr(VI) species must be electroinactive and the concentration of the reducible species must be proportional to the sulphate concetration. Thus, for example, the electroactive species could be a complex of Cr(VI) with sulphate ion as a ligand but the chemical nature of such an interaction is quite unclear. It should also be noted that the calculations of diffusion coefficient assume that migration of sulphate is negligible, i.e. charged chromium species and protons formed by reaction of CrO_3 with water act as the base electrolyte.

Hence there is little doubt that process A is the reduction of Cr(VI) to Cr(III) and that the limiting current for this process is determined by the transport of sulphate to the surface. It must also be recognised, however, that the overall I–E characteristic and particularly the current negative to the peak does not always show the simple behaviour expected for such a process and it varies with the material of the electrode. The deviations are particularly strong under conditions of forced convection when the I–E curves never have the expected simple S-shape. Figures 8–10 show the I–E curves as a function of rotation rate for copper, nickel and carbon electrodes. The results

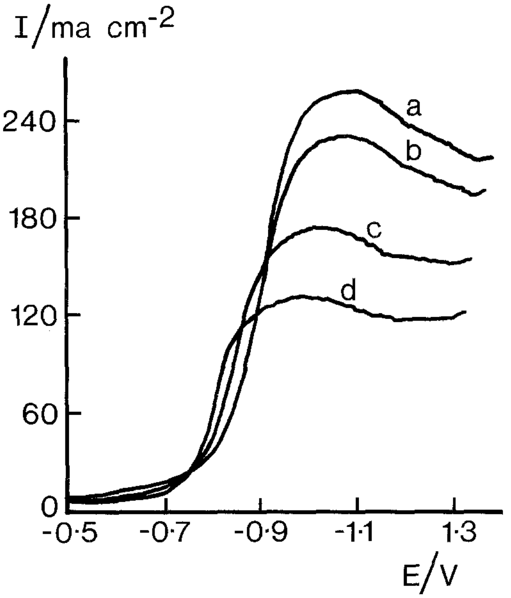

Fig. 8. *I–E* curves at a rotating copper disc electrode. (d) 5 Hz, (c) 10 Hz, (b) 20 Hz, (a) 30 Hz. Potential scan rate 0.01 V s^{-1}. Solution 200 g dm^{-3} CrO_3 + 2 g dm^{-3} H_2SO_4.

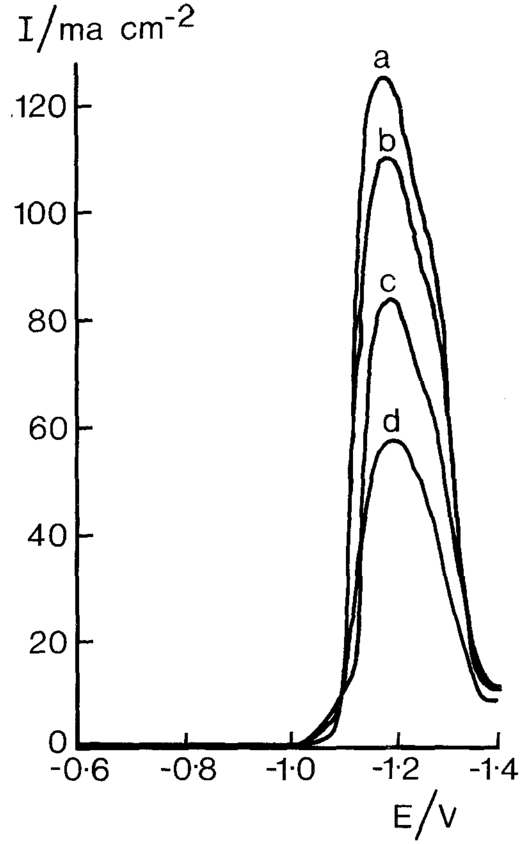

Fig. 9. *I–E* curves at a rotating Ni disc electrode. All other conditions as Fig. 8.

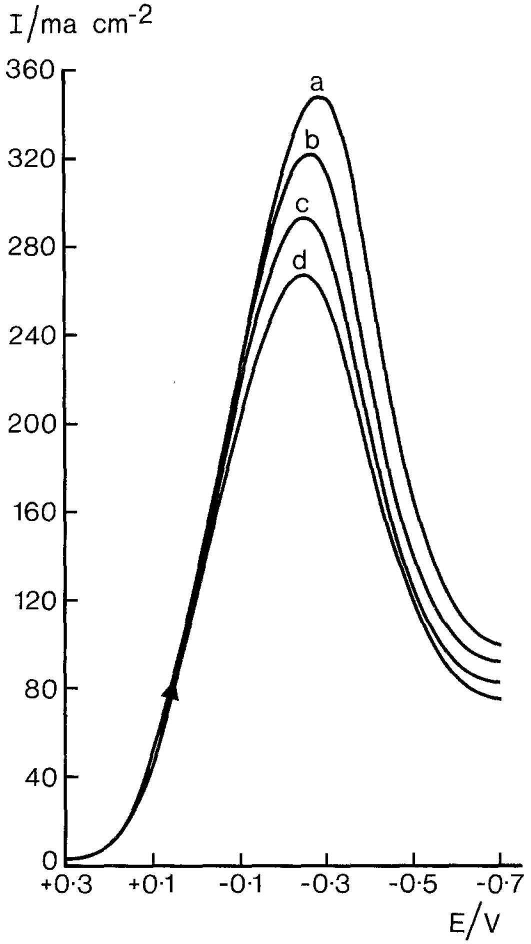

Fig. 10. *I–E* curves at a rotating vitreous carbon electrode. All other conditions as Fig. 8.

at Cu approximate to simple behaviour but the curves at Ni and C show large dips in the potential range where mass transport limited plateaux are to be expected. Two factors may contribute to this behaviour. Firstly, passivation of the surface by films containing chromium ions. The formation of Cr(III) in the presence of sulphate ions will lead to a soluble species but if the rate of production of Cr(III) exceeds the supply of sulphate, it is possible to envisage the formation of chromic dichromate or chromic chromate [$Cr_2(Cr_2O_7)_3$ or $Cr_2(CrO_4)_3$] which will presumably act as insoluble mixed oxide films. Oxide or hydroxide films are also likely to form at potentials where hydrogen evolution leads to an increase in pH close to the cathode surface. Indeed, the curves at Ni show a downward inflection at the potential where hydrogen is evolved (see Fig. 9); Ni is the best hydrogen evolution catalyst of the metals studied and hence is the metal where chromium oxide is most likely to form. The second factor is a double layer effect since the reducible chromium(VI) species is likely to be an anion and hence it may become more difficult to reduce with increasing negative potential under some conditions c.f. the reduction of anions at Hg [21, 22].

What is the relevance of the results in this paper to practical chromium electroplating? Firstly they explain why the sulphate concentration must be low. For chromium plating to occur the electrode potential must reach about − 1.7 V and in the normal controlled current situation, this will only be possible if the current employed is higher than the limiting value for process A (otherwise all the current will be taken up in reduction of Cr(VI) to Cr(III)). Hence the limiting current for process A and consequently the concentration of sulphate must be kept below a critical value. On the other hand, it was found that sulphate ion or another appropriate anion is essential for chromium plating to occur. No metal deposition was seen from a bath containing CrO_3 alone; nor is peak A obtained on *I–E* curves for Ni, Cu or Cr in such solutions, only current for hydrogen evolution is observed. On the other hand, peak A for a C electrode is almost the same as in the presence of H_2SO_4, see Fig. 11. What is the role of the sulphate? It is probable that the anion is necessary for the breakdown of the passivating film on the electrode formed when it is immersed in the bath. The sulphate ion may also play an essential part in providing a lower energy pathway for the reduction of Cr(VI) to Cr(O).

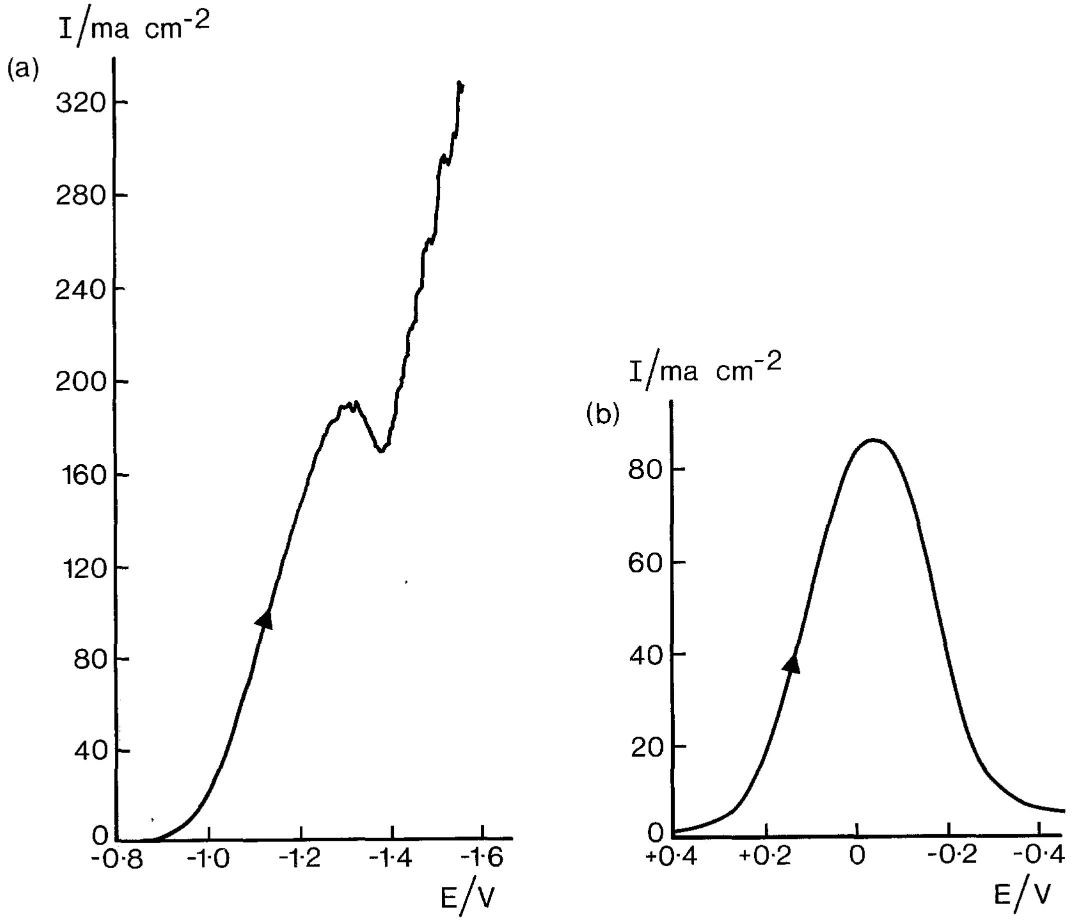

Fig. 11. *I–E* curves at stationary (a) Ni, (b) vitreous C electrodes for a solution of 200 g dm^{-3} CrO_3 only.

4. Conclusions

In a chromium electroplating solution, the electrode reaction occurring at most positive potentials is the reduction of Cr(VI) to Cr(III).

The limiting current density for this process is determined by the transport of sulphate ions to the electrode surface.

At Ni, Cu and Cr electrodes, the potential of the Cr(VI)/Cr(III) couple is determined by the reduction of a passivating film formed spontaneously when the metals are immersed in the bath.

References

[1] 'Canning Handbook of Electroplating', E. and F. N. Son, London, 22nd Edition, (1978).
[2] 'Modern Electroplating', (edited by F. A. Lowenheim), Chapman and Hall, London (1974).
[3] J. K. Dennis and T. E. Such, 'Nickel and Chromium Plating', Newnes-Butterworths, London, (1972).
[4] G. Dubpernell, 'The Electrodeposition of Chromium from Chromic Acid Solutions', Pergamon Press, Oxford, (1977).
[5] H. Gerischer and M. Käppel, *Z. Elektrochem.* **61** (1957) 463.
[6] *Idem, Z. Physik. Chemie* **20** (1959) 83.
[7] *Idem, Z. Elektrochem.* **64** (1960) 235.
[8] D. N. Usachev, *Russ. J. Phys. Chem.* 38 (1964) 501.
[9] *Idem, ibid.* **39** (1965) 256.
[10] N. A. Karnaev, A. G. Mokhov, S. S. Savel'ev and A. I. Levin, *Sov. Electrochem.* **5** (1969) 1299.
[11] T. Inui and T. Fujimoto, *Kinzoku Hyomen Gijutsu,* **23** (1972) 525.
[12] K. Yoshida, A. Suzuki, K. Doi and K. Arai, *ibid.* **30** (1979) 338.
[13] H. Kimura and T. Hayashi, *Denki Kagaku Oyobi Kogyo Butsuri Kagaku,* 37 (1969) 223.
[14] *Idem, ibid.* 37 (1969) 514.
[15] *Idem, ibid.* 38 (1970) 514.
[16] *Idem, ibid.* 39 (1971) 424.
[17] *Idem, ibid.* 39 (1971) 642.
[18] J. P. Hoare, *J. Electrochem. Soc.* **126** (1979) 190.
[19] F. Mullerk and R. Rogers, *ibid.* **68** (1935) 391.
[20] F. Ogburn and A. Brenner, *ibid.* **96** (1949) 347.
[21] R. de Levie and N. Nemes, *J. Electroanal. Chem.* 59 (1975) 123.
[22] P. Delahay 'Double Layer and Electrode Kinetics', Interscience, New York, (1965).
[23] Z. A. Soleveva and A. T. Vagramyan, *Russ. J. Phys. Chem.,* 36 (1962) 392.